A study on the Effects of Convective Momentum Transport Associated with Rain Bands within the Madden-Julian Oscillation

Tomoki Miyakawa [1], Yukari Takayabu [1,2], Tomoe Nasuno [2], Hiroaki Miura [1], Masaki Satoh [1,2]
1. AORI (CCSR), University of Tokyo 2. JAMSTEC

Upscale effects from unresolved Mesoscale Convective Systems (MCSs) are known sources of uncertainty in General Circulation Models (GCMs), which show general difficulty in reproduction of MJOs. The Non-hydrologiccal ICosahedral Atmospheric Model (NICAM) successfully reproduced an MJO case using extremely fine mesh, directly resolving MCSs without cumulus parameterization.

We analyzed the upscale effect of Convective Momentum Transport (CMT) associated with rainbands of MCSs embedded within the convectively active region of the reproduced MJO case. The upscale zonal acceleration ensemble of CMT formed a three-storied structure: positive near the surface (below 1.6km) ; negative at low to mid levels (2km – 6.5km) ; positive at upper levels (above 11km). CMT accounted for -160% of the 2km – 6.5km averaged wind difference that occur associated with the MJO, suggesting that exclusion of CMT effect may result in larger propagation speed of the convective region, possibly up to 10 -15 m/s according to a simplified estimation.

1. NICAM MJO Experiment

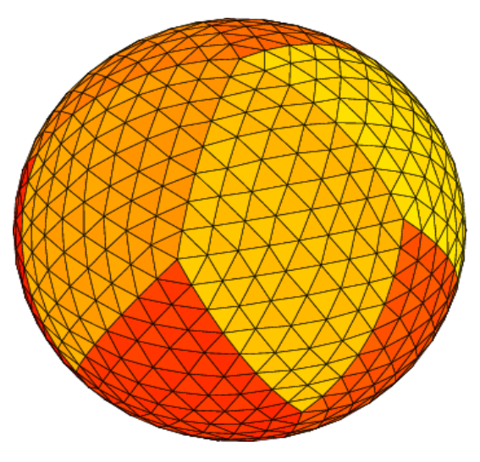

Icosahedral grid used in NICAM (Satoh et al. 2008)

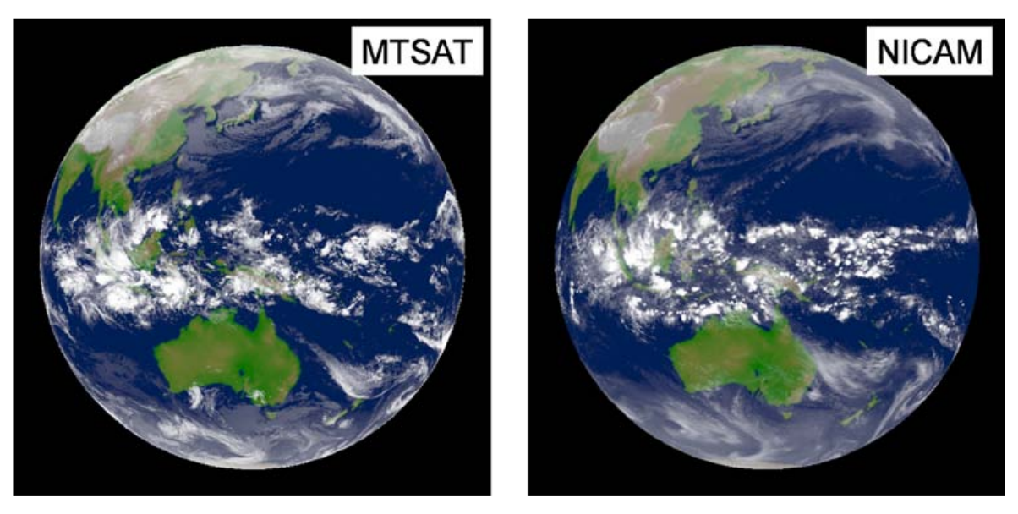

MJO cloud clusters observed from satellite and reproduced by NICAM (Miura et al. 2007).

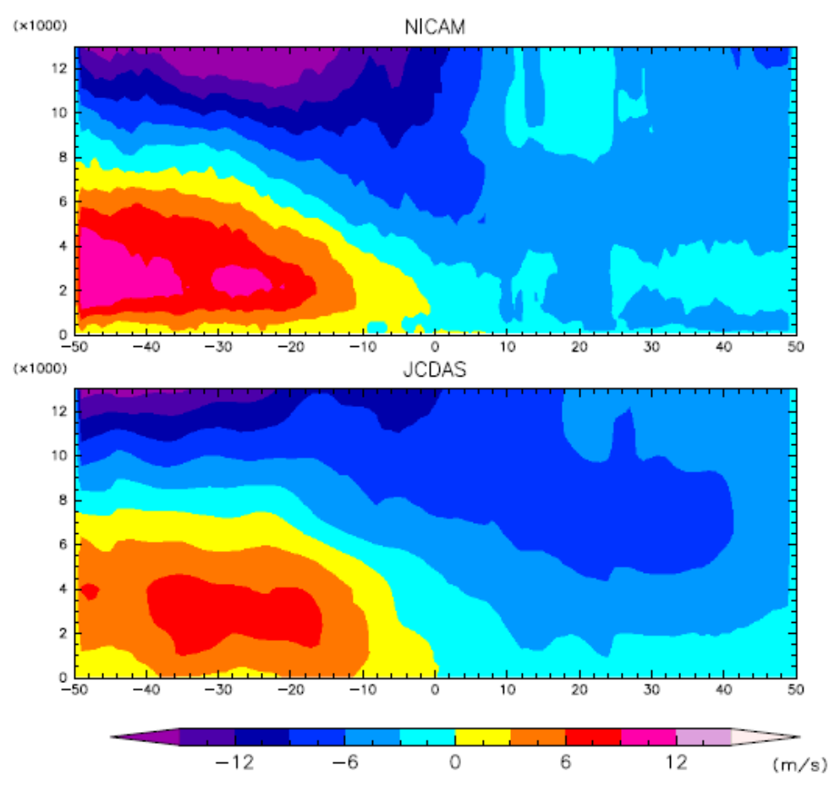

Composed zonal wind structure of the MJO. NICAM (above) and JCDAS-reanalysis (below). The center of the MJO is determined following the EOF based procedure described in Wheeler and Hendon (2004).

NICAM succeed to reproduce an MJO case observed during Dec 2006 – Jan 2007 with surprisingly high accuracy by explicitly representing mesoscale convections without cumulus parameterization (Miura et al. 2007).

In this study we use the 7km mesh output data. Three (two) dimensional data are 6 (1.5) -hourly.

Horizontal grid	Icosahedral grid 7km (3.5km 14km)
Vertical grid	σ-coordinate, Lorenz grid 40 layers 0m ～ 38km
Duration	32 days
Governing equations	Full compressible, Nonhydrostatic
Cumulus parameterization	None
Turbulence / Surface flux	Mellor Yamada - level 2 ＋ water vapor
Radiation / Aerosols	MSTRNX (Sekiguchi 2004)
Cloud microphysics	Grabowski(1998)
Surface process	Bucket land model / Fixed SST
Initial condition	NCEP – Reanalysis 2006-12-15 00:00:00
Boundary conditions	Reynolds SST, Sea Ice (weekly) E-topo5 topography, Matthews vegetation UGAMP ozone climatology (for AMPI2)

Model configuration for the MJO experiment.

2. Upscale Convective Momentum Transport within the MJO

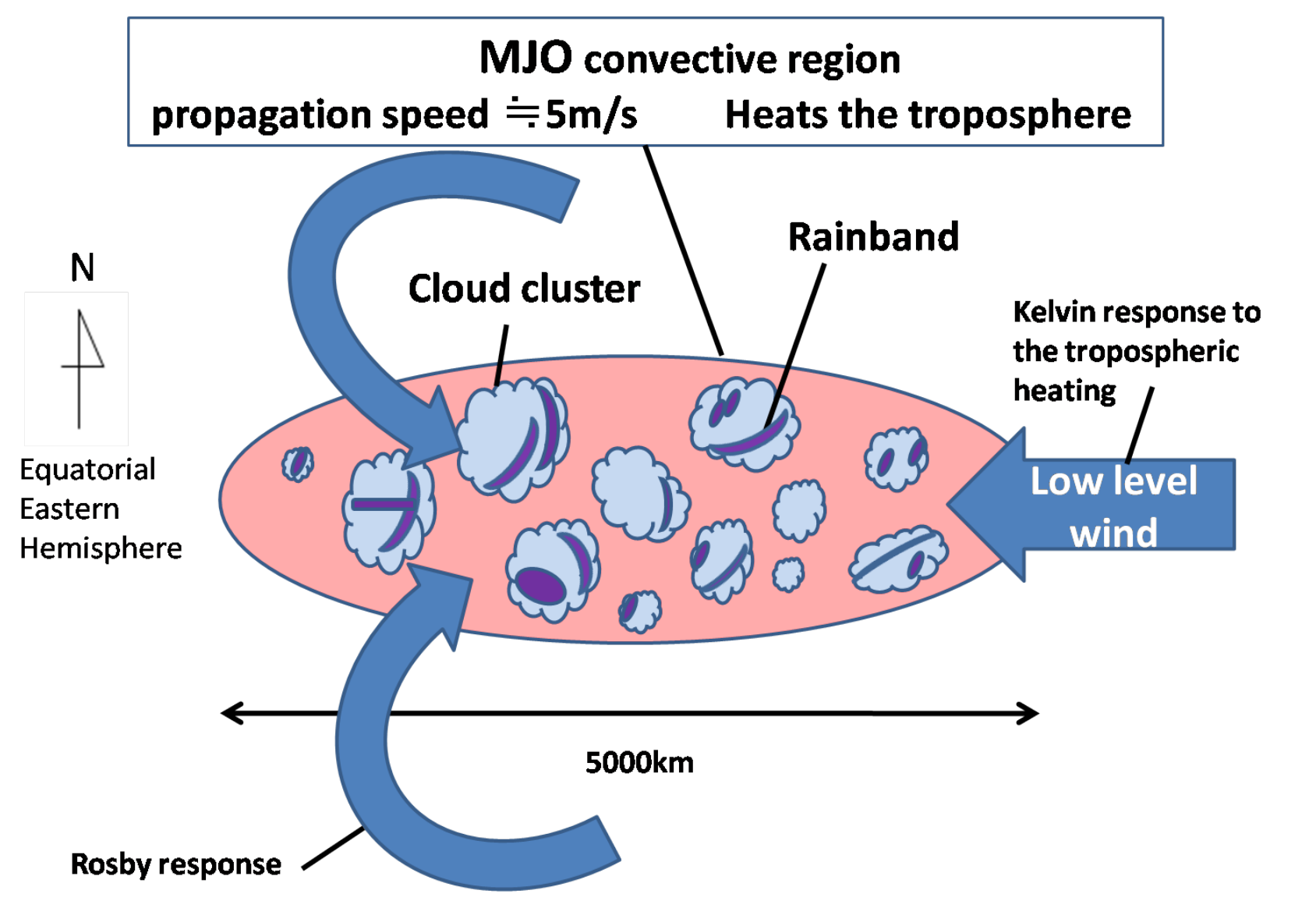

Schematic structure of MJO and embedded convection. Arrows show the Matsuno-Gill type response due to the cumulus heating ensemble. This study stands in the point of view that eastward propagation of the MJO is controlled by the eastward shift of the region favorable for convection.

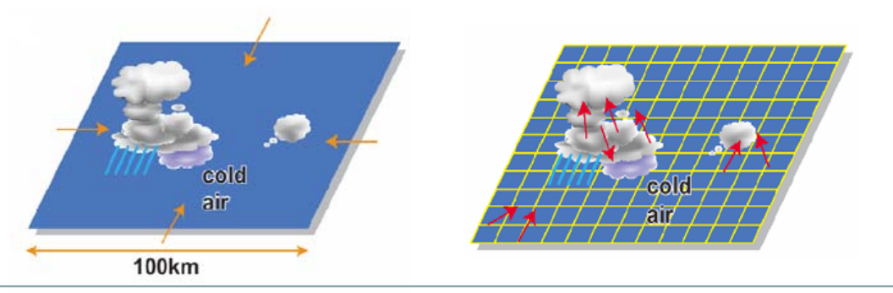

Schematic showing the relation between mesoscale convection and grids of typical GCM (left) and NICAM (right).

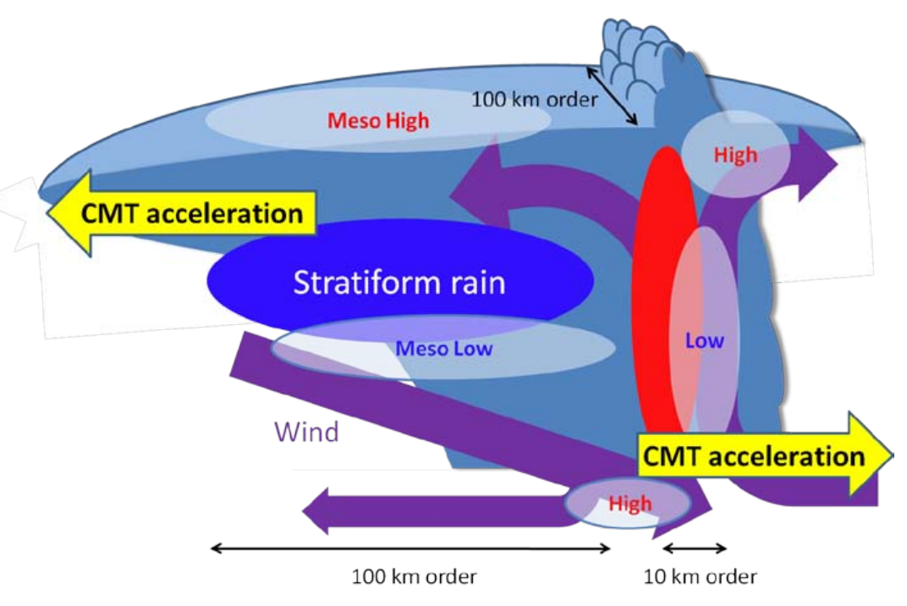

Schematic of a typical squall-line type MCS. Momentum flux divergence (acceleration due to CMT), affected by the horizontal pressure gradient across the vertical flow, can have counter gradient effects on the vertical wind shear when the convection are organized in to a linear structure.

CMT associated with rainbands embedded in MJOs cause upscale acceleration. This effect is usually parameterized as sub-grid mixing components in GCMs. However, it is known from observation and numerical experiments that organized rainbands can have counter gradient effects on the vertical wind shear (e.g. LeMone and Moncrieff, 1994; Tung and Yanai 2002).

3. Rainbands Detected in the NICAM MJO case

Threshold used for rainband detection : (Size of continuous area where precipitation≧0.3mm/h) ≧ 500km²

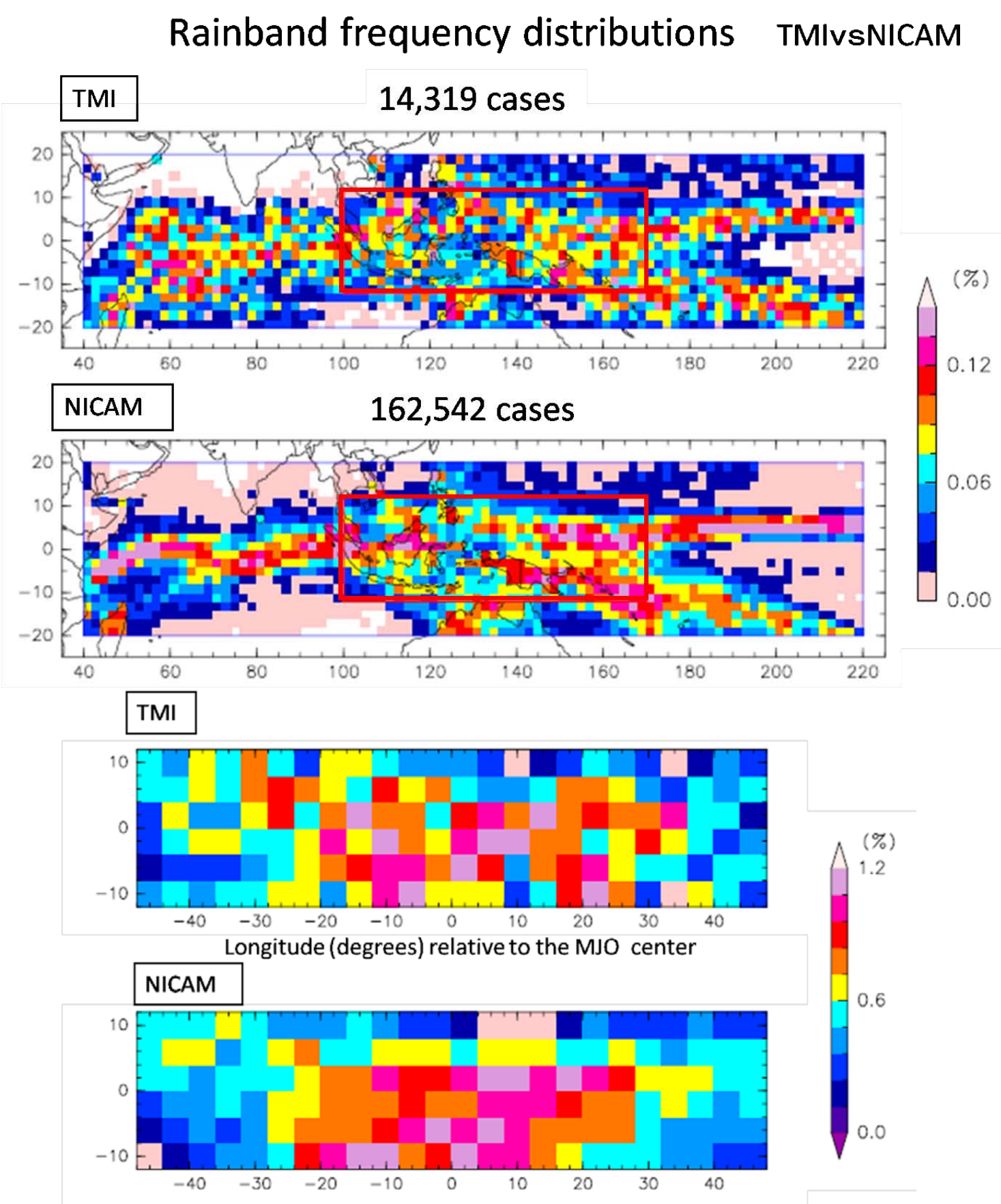

Rainband frequency distribution map derived from TMI and NICAM (above). The expected ratio of rainband case numbers estimated from the data retrieval difference is about 10 – 15. Red rectangle indicates the main analysis region used hereafter in this study. The lower figure shows the spatial distribution of rainbands relative to the MJO center.

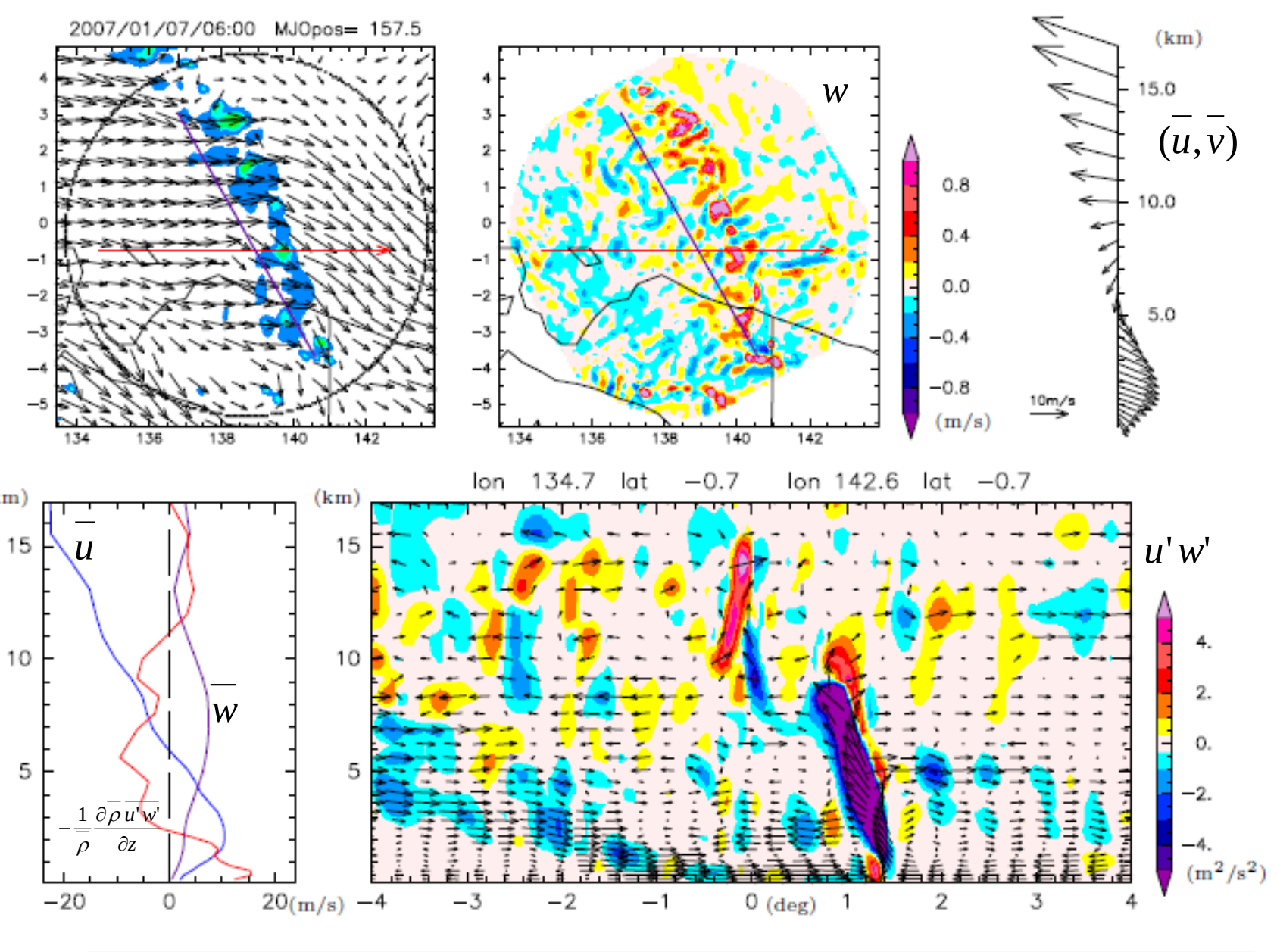

An example of an ideal squal l-line type rainband produced in NICAM. Upper left figure shows the surface rainfall (color) and zonal wind vectors at 1580m height. Upper central figure shows the vertical wind within the region determined to be under the influence of the rainband. Upper right figure shows the vertical profile of $(\overline{u},\overline{v})$, the horizontal wind averaged over the circle indicated in the upper left figure. The lower left figure show vertical profiles of : $\overline{u}$ (blue) ; $\overline{w}$ (purple) ; and upscale acceleration by $-\frac{1}{\overline{\rho}}\frac{\partial \overline{\rho}\,\overline{u'w'}}{\partial z}$ (red) . The lower right figure is a zonal-height cross section of $u'w'$. The red arrow in the upper left figure indicates the zonal axis of the lower right figure.

Total number and frequency distribution of rainbands produced in NICAM are consistent with satellite data (TRMM/TMI) considering data retrieval differences. The area within 100°E - 170°E / 12°N – 12°S (red box), where the cases are abundant and the distribution agree well, is chosen as the main analysis region.

While some ideal squall line type rainbands are found (upper right figure), there were many cases with complicated structures (not shown).

4. Distribution of CMT Acceleration Vectors

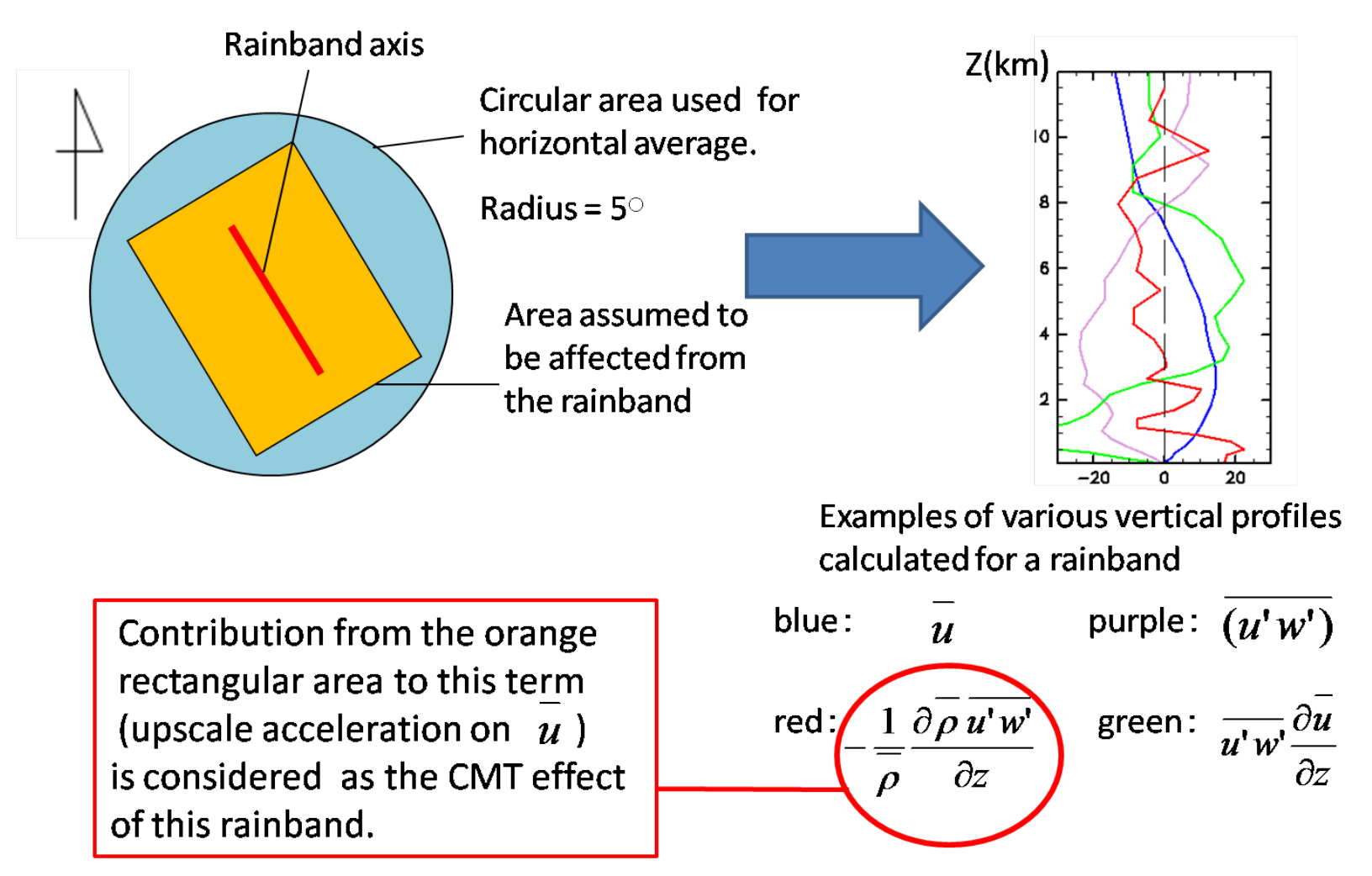

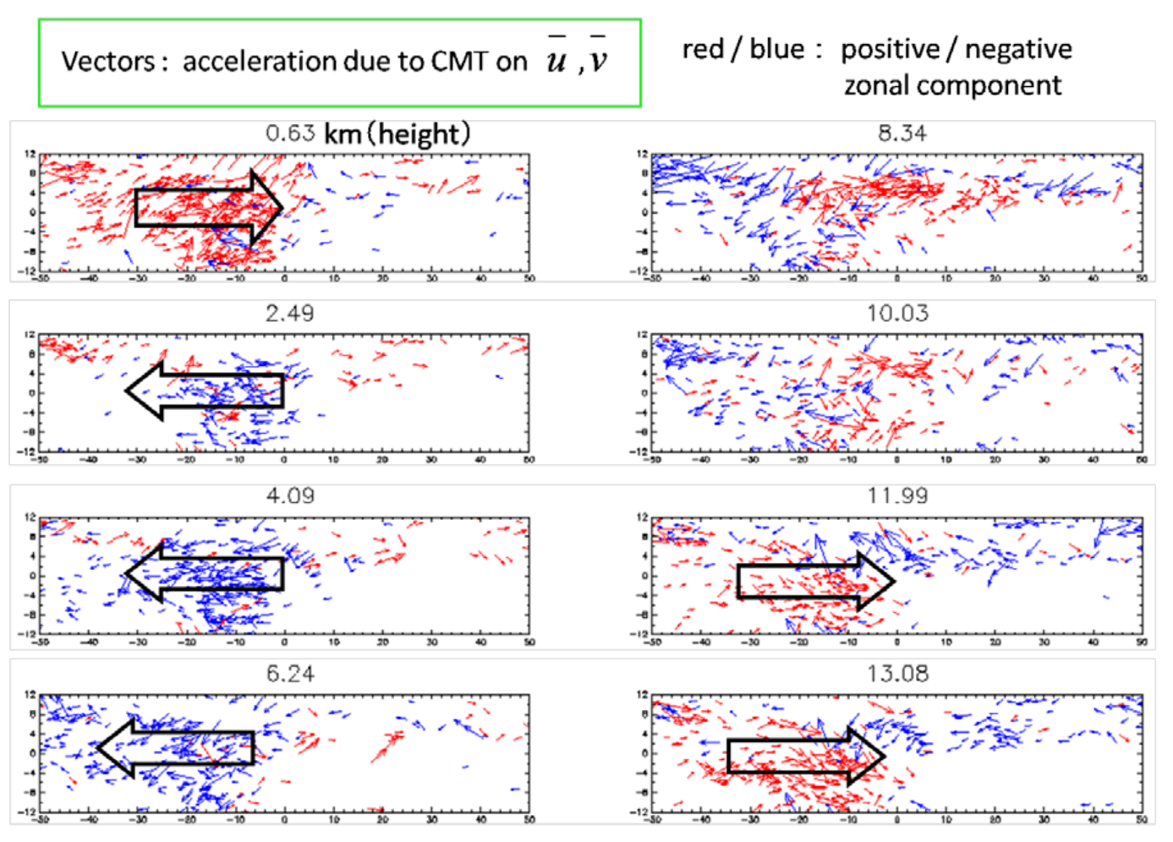

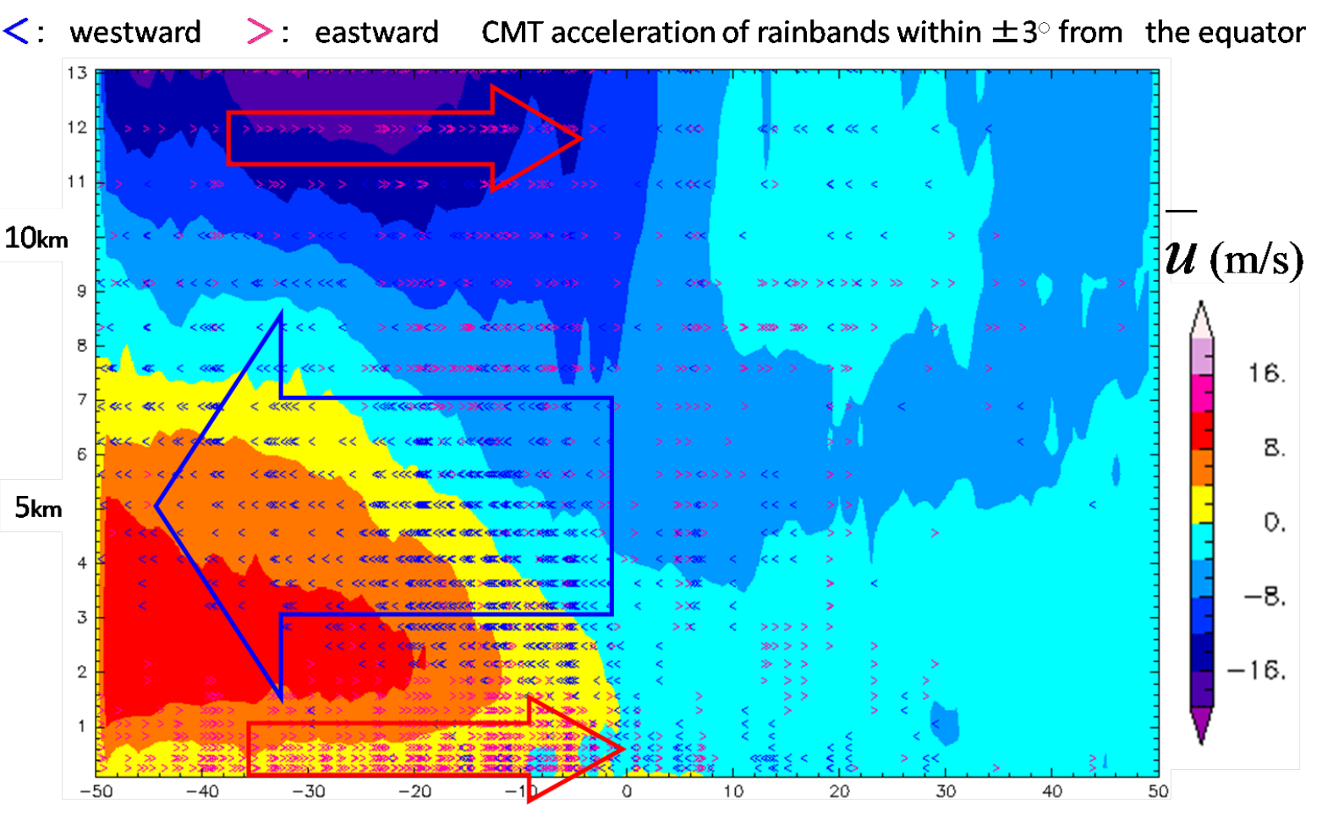

MJO relative distribution of upscale CMT acceleration vectors defined by the deviation momentum flux divergence shows a three storied structure : positive zonal component near the surface (below 1.6km) ; negative zonal component at low to mid troposphere (2km-6.5km) ; positive zonal component at the upper troposphere (above 11km).

Plan view (above) and zonal-height cross section (below, colors show $\overline{u}$) of CMT vector distribution relative to the MJO center.

5. Quantitative Evaluation of Upscale Acceleration due to CMT

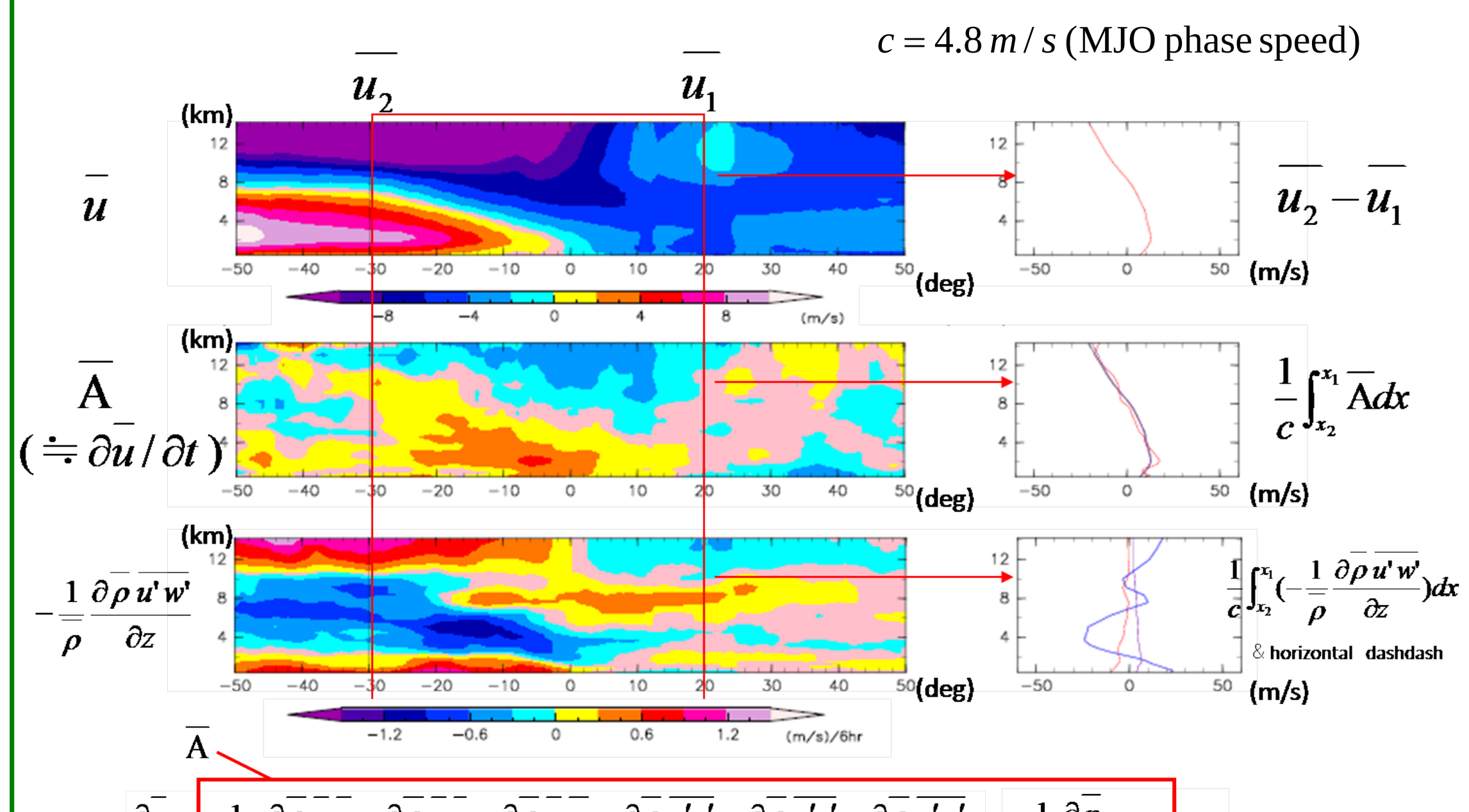

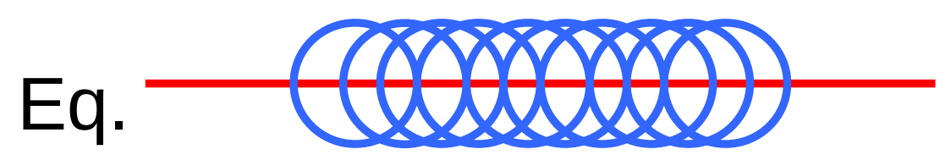

$$\frac{\partial \overline{u}}{\partial t} = \boxed{-\frac{1}{\overline{\rho}}\left(\frac{\partial \overline{\rho}\,\overline{u}\,\overline{u}}{\partial x}+\frac{\partial \overline{\rho}\,\overline{u}\,\overline{v}}{\partial y}+\frac{\partial \overline{\rho}\,\overline{u}\,\overline{w}}{\partial z}+\frac{\partial \overline{\rho}\,\overline{u'u'}}{\partial x}+\frac{\partial \overline{\rho}\,\overline{u'v'}}{\partial y}+\frac{\partial \overline{\rho}\,\overline{u'w'}}{\partial z}\right) - \frac{1}{\overline{\rho}}\frac{\partial \overline{p}}{\partial x} + f\overline{v}} + \overline{F}$$

Figures on the left row are MJO relative composites of zonal-height cross sections achieved by aligning vertical profiles calculated in each 5° radius circle distributed over the equator (above). Figures on the right row compare the difference and the integrated tendency terms of the mean zonal wind between 20° and -30° from the MJO center. MJO phase speed c is assumed to be constant and is derived following WH04.

By distributing the 5° radius circles evenly over the equator, quantitative evaluation of upscale acceleration due to $-\frac{1}{\overline{\rho}}\frac{\partial \overline{\rho}\,\overline{u'w'}}{\partial z}$ is performed. $-\frac{1}{\overline{\rho}}\frac{\partial \overline{\rho}\,\overline{u'w'}}{\partial z}$ has significant contribution to the wind difference between 20° and -30° from the MJO center. In the low to mid troposphere (2km-6.5km), its contribution on the zonal wind difference was as much as -160% in average.

6. Discussion on the Roles of CMT

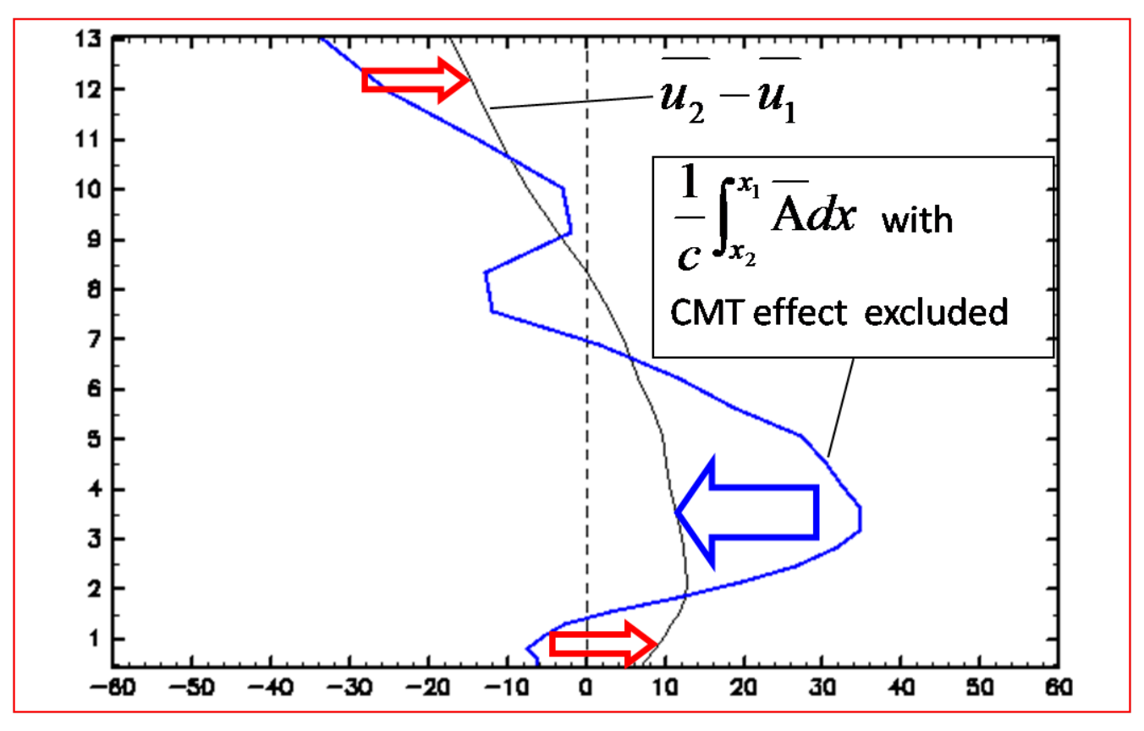

Integrated tendency of the mean zonal wind with CMT effect excluded. Arrows indicate CMT effects.

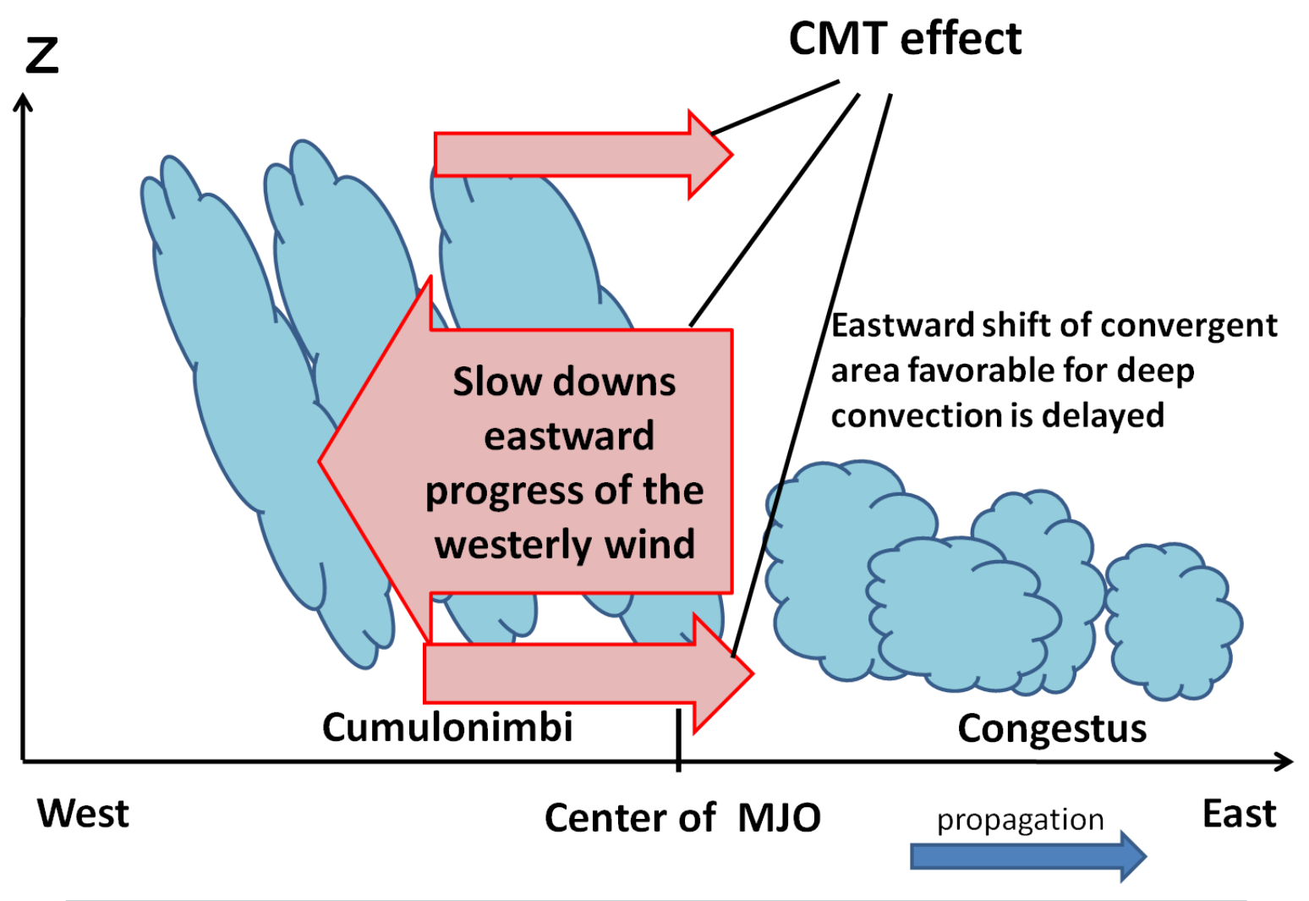

A schematic describing the suggested role of CMT effect.

From the point of view that eastward propagation is controlled by the eastward shift of favorable region for convection, we state further assumptions as follows : (1) development of new convection following the eastward shift of the favorable region and the Matsuno-Gill response occur instantaneously; (2) the MJO wind structure does not change when CMT effects are excluded.

Then, when CMT effects are excluded, the eastward progress of the low to mid level westerly wind speeds up by 260%, thereby speeding up the eastward shift of low to mid level convergent area favorable for deep convection. New convection develops and the MJO wind structure follows instantaneously, and the phase speed of the entire MJO also speeds up by 260%.

Although this estimation is possibly over-simplified, it demonstrates that the impact can be large, and suggests that sufficient representation of mesoscale convections are required for accurate MJO reproduction (In order to do a more realistic estimation, a numerical experiment is required) .